Histol Histopathol (2008) 23: 67-76

http://www.hh.um.es

Histology and Histopathology

Cellular and Molecular Biology

Aß deposition and related pathology in an APP x PS1 transgenic mouse model of Alzheimer's disease

D.R. Howlett, K. Bowler, P.E. Soden, D. Riddell*, J.B. Davis, J.C. Richardson, S.A. Burbidge, M.I. Gonzalez, E.A. Irving, A. Lawman, G. Miglio#, E.L. Dawson, E.R. Howlett, I. Hussain

Neurology & GI CEDD, GlaxoSmithKline, Harlow, Essex, UK. Present adresses: *Wyeth Research, Princeton, NJ, USA and #DISCAFF Department, University of Piemonte Orientale, Novara, Italy

Summary. A transgenic mouse bearing mutant transgenes linked to familial forms of Alzheimer's disease (AD) for the amyloid precursor protein and presenilin-1 (TASTPM) showed Aß plaque deposition and age-related histological changes in associated brain pathology. The Aß present was of multiple forms, including species with a C-terminus at position 40 or 42, as well as an N-terminus at position 1 or truncated in a pyro-3-glutamate form. Endogenous rodent Aß was also present in the deposits. Laser capture microdissection extracts showed that multimeric forms of Aß were present in both plaque and tissue surrounding plaques. Associated with the Aß deposits was evidence of an inflammatory response characterised by the presence of astrocytes. Also present in close association with the deposits was phosphorylated tau and cathepsin D immunolabelling. The incidence of astrocytes and of phosphorylated tau and cathepsin D load showed that both of these potential disease markers increased in parallel to the age of the mice and with Aß deposition. Immunohistochemical labelling of neurons in the cortex and hippocampus of TASTPM mice suggested that the areas of Aß deposition were associated with the loss of neurons. TASTPM mice, therefore, exhibit a number of the pathological characteristics of disease progression in AD and may provide a means for assessment of novel therapeutic agents directed towards modifying or halting disease progression.

Key words: Amyloid precursor protein, Alzheimer's disease, Beta-amyloid

Offprint requests to: D.R. Howlett, Neurology & GI CEDD, GlaxoSmithKline, Harlow, Essex, CM19 5AD, UK. e-mail: david.r.howlett@gsk.com

Introduction

The brains of patients with Alzheimer's disease (AD) are characterised by the presence of Aß plaques and neurofibrillary tangles, first described by Alois Alzheimer a century ago. There is also extensive, cortical atrophy, neuronal damage and loss which can approach 25% in affected areas of cortex (Mann, 1991; Braak et al., 2006). The loss of cortical neurons, particularly of the large pyramidal neurons of layers II and IV, relates directly to the cognitive decline seen in AD (Mouton et al., 1998). Thus, to be a viable model of AD, any animal model would be expected to exhibit some degree of atrophy and neuronal loss, as well as plaque and tangle pathology.

Familial forms of AD are associated with mutations in the APP and presenilin genes (for review see Selkoe and Podlisny, 2002). This knowledge has, therefore, been utilised to generate potential animal models of AD. A number of mouse models have been reported overexpressing mutant human APP transgenes, including human APPswe (Sturchler Pierrat et al., 1997; Kawarabayashi et al., 2001), APP London (Dewachter et al., 2000), APP Indiana (Games et al., 1995) and APPswe+London (Chishti et al., 2001; Schmitz et al., 2004). In some cases these transgenes have been combined with those for mutant human presenilin-1 (Borchelt et al., 1997; Holcomb et al., 1998; Kurt et al., 1999; Dewachter et al., 2000) to produce accelerated deposition of Aß. The overexpression of a single human mutant APP transgene typically results in cerebral plaque-like ß-amyloid (Aß) deposits from approximately 12 months of age (Hsiao et al., 1996; Richardson et al., 2003). Possession of human double mutant APP transgenes gives rise to cerebral Aß deposits from 3-4 months of age (Chishti et al., 2001). Mice bearing both mutant human APP and PS-1 transgenes also exhibit plaques from as early as 3 months of age (Holcomb et

al., 1998; Kurt et al., 2001).

The TASTPM mouse expresses both human APPswe and PS-1.M146V transgenes and has been shown to deposit Aß from 4 months of age (Howlett et al., 2004). In this report we explore the pathology associated with the Aß deposition in the TASTPM model and describe features, including neuronal cell loss, characteristic of AD.

Materials and methods

Mice

Transgenic mice over-expressing the hAPP695swe mutation (TAS10) and transgenic mice over-expressing the presenilin-1 M146V mutation (TPM) were generated as previously described (Richardson et al., 2003). TAS10 (Thy-1.APPswe) mice were generated and backcrossed onto a pure c57bl/6 background before crossing with TPM (Thy-1.PS-1.M146V) mice to produce heterozygote double mutant mice (TASTPM) (Howlett et al., 2004). Non-transgenic litter mates were used as controls where appropriate.

Antibodies

Aß was detected with: FCA18 (Calbiochem), specific for Aß 1-x; 6E10 (Signet), a pan-Aß antibody; monoclonal 1E8 (2.4 µg/ml) raised against the 13-27 fragment of Aß (Allsop et al., 1997); monoclonal 20G10 (0.28 mg/ml) raised against the Aß35-42 fragment and selected for its C-terminal Aß42 specificity; rabbit antiserum G30 (3 mg/ml) raised against CMVGGVV for Aß40 (Howlett et al., 2004); rodent Aß was detected with an in-house polyclonal raised to the rodent Aß 1-16 fragment. Rodent specificity of this antibody was established by pre-incubation of the antibody with a ten-fold excess of the rodent Aß 1-40 peptide (Anaspec), which completely obliterated the labelling of amyloid deposits in sections of double transgenic mouse brain. In contrast, pre-incubation of the rodent Aß antibody with human Aß 1-40 peptide (California Peptide Res Inc) had no discernible effect on immunolabelling. Furthermore, the rodent Aß antibody showed no labelling of Aß plaques in human brain sections. N-terminally truncated Aß was detected with a pyro-3-glutamate-Aß antibody (IBL, Hamburg). Other antibodies used: GFAP (Dako), AT8 (Innogenetics), cathepsin D (Santa Cruz), NeuN (Zymed) and Iba1 (Wako Chemicals).

Aß concentration

Male TASTPM mice were humanely sacrificed at various ages by intraperitoneal injection of a lethal dose of pentobarbitone sodium (Euthatal, Rhone Merieux, Harlow, UK). Routinely, the brains were hemisected, the left half being collected into pre-weighed 2ml Eppendorf™ tubes and immediately snap frozen for biochemical assessment of Aß concentrations. Samples were subsequently thawed, reweighed and 1 ml of 5M guanidine HCl containing Complete protease inhibitor tablets (Boehringer Mannheim) added, before the samples were homogenized and incubated at 4°C for 90 minutes with constant agitation. Samples were subsequently diluted 1 in 10 into assay buffer (50 mM Tris HCl, pH7.4, 150 mM NaCl, 0.05% Tween-20 + 1% BSA) to give a final volume of 1ml, vortexed and spun at 20,000g for 20 mins at 4°C. The supernatant was removed and added as triplicate samples to the assay plate. Samples were assayed for Aß40 or Aß42 using a sensitive BioVeris™ immunoassay employing Aß C-terminal specific antibodies. Briefly, Aß peptides were captured using biotinylated 6E10 (Signet Laboratories). C-terminal Aß40 (G210; The Genetics Company) and Aß42 (5G5; raised to C-terminal Aß residues MVGGVVIA) antibodies labelled with a BVTM Ruthenium NHS ester tag were used to detect the specific Aß species. Antibody-Aß complexes were captured with streptavidin coated Dynabeads® (Dynal) and assayed in a BioVerisTM M384 analyser.

Immunohistochemistry

The right half of each hemisected brain was immersed in 4% paraformaldehyde for 72 hours before being processed into paraffin wax. Serial 5 µm sections were cut and subjected to standard immuno-histochemical techniques. Briefly, the sections were de-waxed, re-hydrated through a series of graded alcohols and washed in distilled water. Sections to be labelled with Aß antibodies were treated with 85% formic acid for 8 min in order to enhance Aß antigenicity. Sections used for NeuN, phosphoTau, GFAP, Iba1 and cathepsin D were microwaved (2x5 minutes at 300 w) in 10mM citrate buffer pH 6.0 to enhance antigen retrieval. Where sections were to be double labelled with an Aß antibody and a second antibody, sections were microwaved in citrate buffer prior to formic acid treatment. All sections were subsequently incubated in 0.3% H_2O_2 in 0.1 M phosphate buffered saline pH 7.4 (PBS) for 30 min at room temperature to quench endogenous peroxidase activity followed by washing (3x5 min) in 0.1M PBS. Sections were subsequently incubated overnight at 4°C with primary antibodies in primary diluent (0.3% Triton-X-100, 0.01% sodium azide and 2% normal serum in PBS). Immunohistochemistry was completed with appropriate secondary biotinylated antibodies (Vector Laboratories Ltd, Peterborough, U.K.) diluted 1:500 in secondary layer diluent (0.3% Triton-X-100 in 0.1M PBS), followed by avidin-biotin complexation (Vector ABC, Vector Laboratories Ltd, Peterborough, U.K.) and visualisation using diaminobenzidine according to the manufacturer's data sheets (Vector Laboratories Ltd, Peterborough, U.K.). In some experiments, nickel enhancement was utilised. Where appropriate, sections were lightly counter-stained with Mayer's haemotoxyllin (Sigma Aldrich). For double labelling experiments, the second primary antibody was visualised with violet

immunoperoxidase (VIP - Vector Laboratories Ltd, Peterborough, U.K.). For triple labelling, visualisation was with DAB, VIP and Vector Blue. Control experiments were run in parallel where either the primary antibodies or both primary and secondary antibodies were omitted to reveal any non-specific labelling produced by the secondary or tertiary layers. Photo images of each section were produced using a Leica DM-RB microscope equipped with a DC100 digital camera and software. Quantification of labelling was achieved using either Qwin (Leica) or ImageProPlus software and was expressed as % area labelled (GFAP) or positive neurite counts (phosphotau).

Laser capture microdissection

Sections were prepared for laser capture microdissection (LCM) by firstly undertaking immunohistochemical labelling with Aß antibodies, exactly as described above with the exception that after clearing with Histoclear®, sections were allowed to air-dry overnight with no mountant or coverslip. Plaque excision was carried out on an Arcturus PixCell II instrument (Arcturus Biosciences Inc., Mountain View, CA) with a beam diameter of 30 µm and beam strength of 100 mW for 25 milliseconds. Dissected tissue was lifted from the sections using Capsure LCM polycarbonate caps (Arcturus Biosciences Inc.). Tissue lifted was typically 30-100 µm in diameter and about 5 µm in thickness. The resolution of the instrument resulted in the dissection of plaque plus small amounts of surrounding tissue. Inter-plaque material was defined as not being labelled with Aß antibodies but was sampled from areas adjacent to plaques. Non-plaque material was dissected from areas such as the caudate nucleus or cerebellum.

Approximately 100 tissues spots were lifted onto a cap. The dissected material on each cap was extracted into 35 µl of SDS sample buffer (NuPage, Invitrogen) by incubating the cap with the buffer overnight at room temperature. Samples were reduced by heating to 70°C for 10 minutes before being applied to a 12% Bis-Tris gel (NuPage, Invitrogen). Gels were subsequently blotted onto nitrocellulose membranes, developed with Aß antibodies and visualised by enhanced chemiluminescent detection (Amersham).

Results

The Aß composition of the plaques in the TASTPM brain was examined with a range of specific antibodies. The plaques were labelled with a pan-Aß + APP antibody (Fig. 1a) and were found to contain Aß forms commencing with Asp1 (Fig. 1b) and ending in the 40 and 42 C-termini (Fig. 1c,d). In each case, the labelling was associated with both the plaque cores and more diffuse material surrounding the core (Fig. 1a-d insets). Although not so plentiful, labelling was also observed

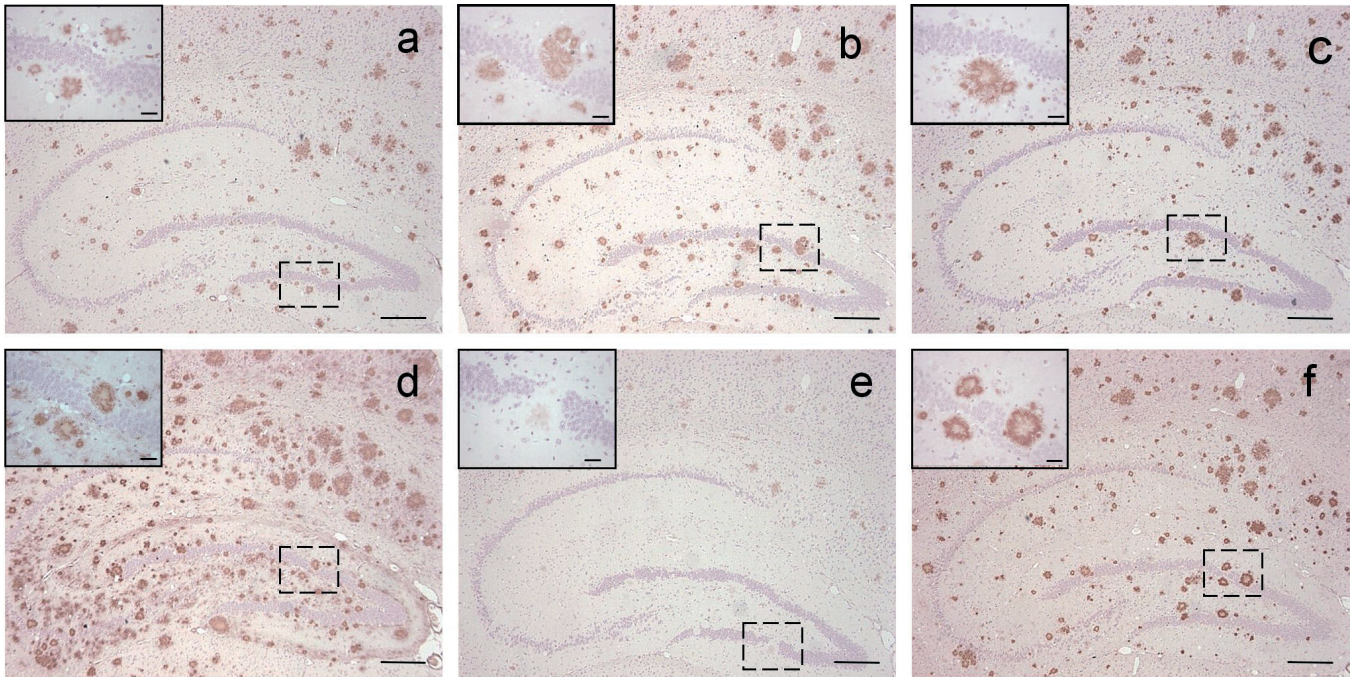

Fig. 1. Immunohistochemical profiling of Aß deposits in the brain of an 81 week TASTPM mouse. Antibody labelling: **(a)** total Aß (antibody 6E10); **(b)** Aß1-x (FCA18); **(c)** Aß x-40 (G30); (**d**) Aß x-42 (20G10); (**e**) pyro-3-glutamate-A; (**f**) rodent Aß. Counter-staining was with Mayer's haemotoxyllin. The scale bars represents 200 microns on the main figures and 25 microns on the insets.

with a specific pyro3-glutamate N-termini Aß antibody, particularly in areas proximal to the hippocampus (Fig 1e). As might be expected in a mouse model bearing human APP transgenes, much of the Aß was of the human sequence and could be labelled with the human specific 6E10 and FCA18 antibodies (Fig. 1a,b). However, a rodent Aß specific antibody also produced plaque labelling (Fig. 1f) showing the presence of endogenous rodent amyloid associated with the deposits.

The immunohistochemical analysis demonstrated the presence of Aß forms of varying lengths but did not provide any information about the aggregation state of the peptide. In an attempt to presence of multimeric species of the Aß forms associated with the plaques and surrounding tissue (ie. tissue from plaque rich areas not showing any obvious Aß immunolabelling), laser capture microdissection was employed to produce plaque enriched extracts and extracts from tissue surrounding the plaques. Western blots showed the presence of bands corresponding to monomeric Aß plus dimers, trimers and higher molecular weight oligomeric species (Fig. 2). Although inter-plaque material contained less Aß, the bands representing the oligomeric species were virtually identical between the different preparations. The Aß present was of both C-terminal 40 (Fig. 2) and 42 forms (data not shown). In contrast, tissue from non-plaque areas (eg. caudate putamen or cerebellum) showed little evidence of Aß bands on the blot. It would therefore appear that focal concentrations of aggregated Aß peptide appear as distinct deposits but that the surrounding tissue, although not possessing sufficient Aß to facilitate immunohistochemical labelling, does, nevertheless contain aggregated Aß forms.

Labelling of neurons with the NeuN antibody clearly showed that areas occupied by amyloid plaques were devoid of neurons (Fig. 3a-c). Double labelling of neurons in the CA1-CA3 and dentate gyrus with NeuN and Aß antibodies showed no evidence of cells being displaced laterally by the amyloid mass (Fig. 3d; see also insets of Fig. 1a-d). This Aß often took the form of a plaque core surrounded by more diffuse labelling (Fig. 3d). Labelling with the pyro-glutamate antibody was less common. In particular, plaques in the hippocampus, around the CA1-3 and dentate gyrus were rarely labelled and the presence of plaques was apparent by the lack of labelling with the pyro-glutamate antibody (arrows in Fig. 3e). This may suggest that neuronal loss is not dependent upon the presence of pyro-3-glutamate truncated Aß. Where labelling was apparent with this antibody, it appeared to be to plaque cores rather than diffuse material, sometimes labelling plaques with multiple cores (Fig. 3f). Labelling of Aß plaques in material from a Braak stage 6 AD subject is shown in Fig. 3g,h. Small, relatively compact Aß42-positive plaques were found in the hippocampus of this subject. Using the cell layers of the hippocampus as a guide, it would appear that neuronal loss in the vicinity of the amyloid plaques in AD brain is very similar to that observed in TASTPM mice (compare Fig. 3c,h).

Inflammatory cells were observed in close proximity to the Aß deposits. GFAP-positive astrocytes were found to be closely associated with the amyloid deposits (Fig. 4a). The association between plaque deposition, GFAP-positive astrocytes and neuronal loss is illustrated in Fig. 4b. Note how the astrocytes infiltrate the neuronal layer of the dentate gyrus. A similar association with Aß deposits was noted for microglia cells labelled with the iba-1 antibody (Fig. 4c - Aß labelling has been omitted for clarity). The belief that cells in the vicinity of the plaques had degenerated was supported by the appearance of high levels of cathepsin D immunoreactivity in close association with the Aß deposits (Fig. 4d).

Aß40 and Aß42 levels were measured in the brains of TASTPM mice from 2 months of age. Levels of both Aß40 and 42 increased from approximately 20 pmoles/g at 2 months of age to around 10 nmoles/g at 8 months

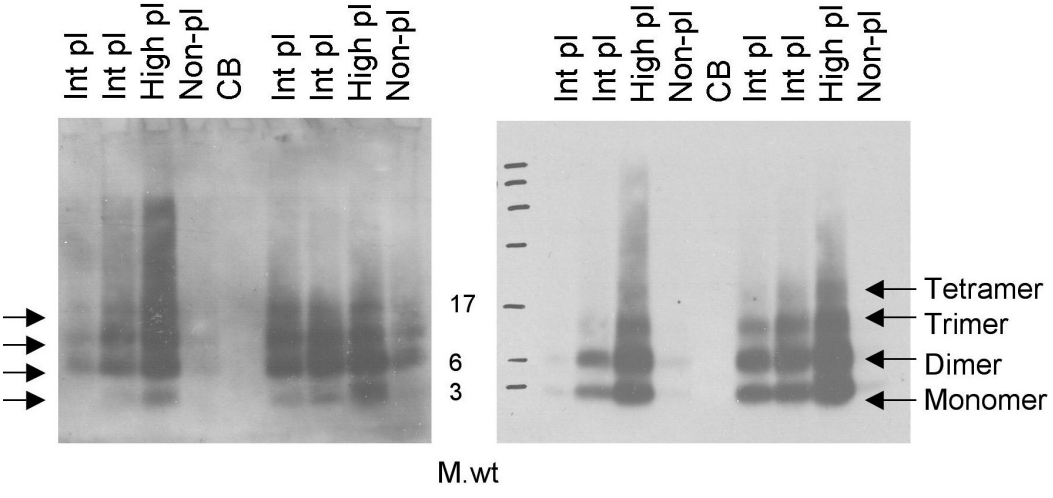

Fig. 2. Western blots of laser capture microdissection extracts of TASTPM brain sections. Blots (left and right, 2 animals per blot) show extracts of high-plaque (High pl), inter-plaque (Int pl) and non-plaque regions (Non-pl) and cerebellum (CB). Microdissected material was extracted into SDS buffer followed by separation using SDS-PAGE and western blotting. Blots above show immunoreactivity with antibody 1E8 (total Aß). The position of molecular weight markers have been shown to allow the probable identification of the oligomeric species of Aß illustrated by the arrows.

(Fig. 5 a).

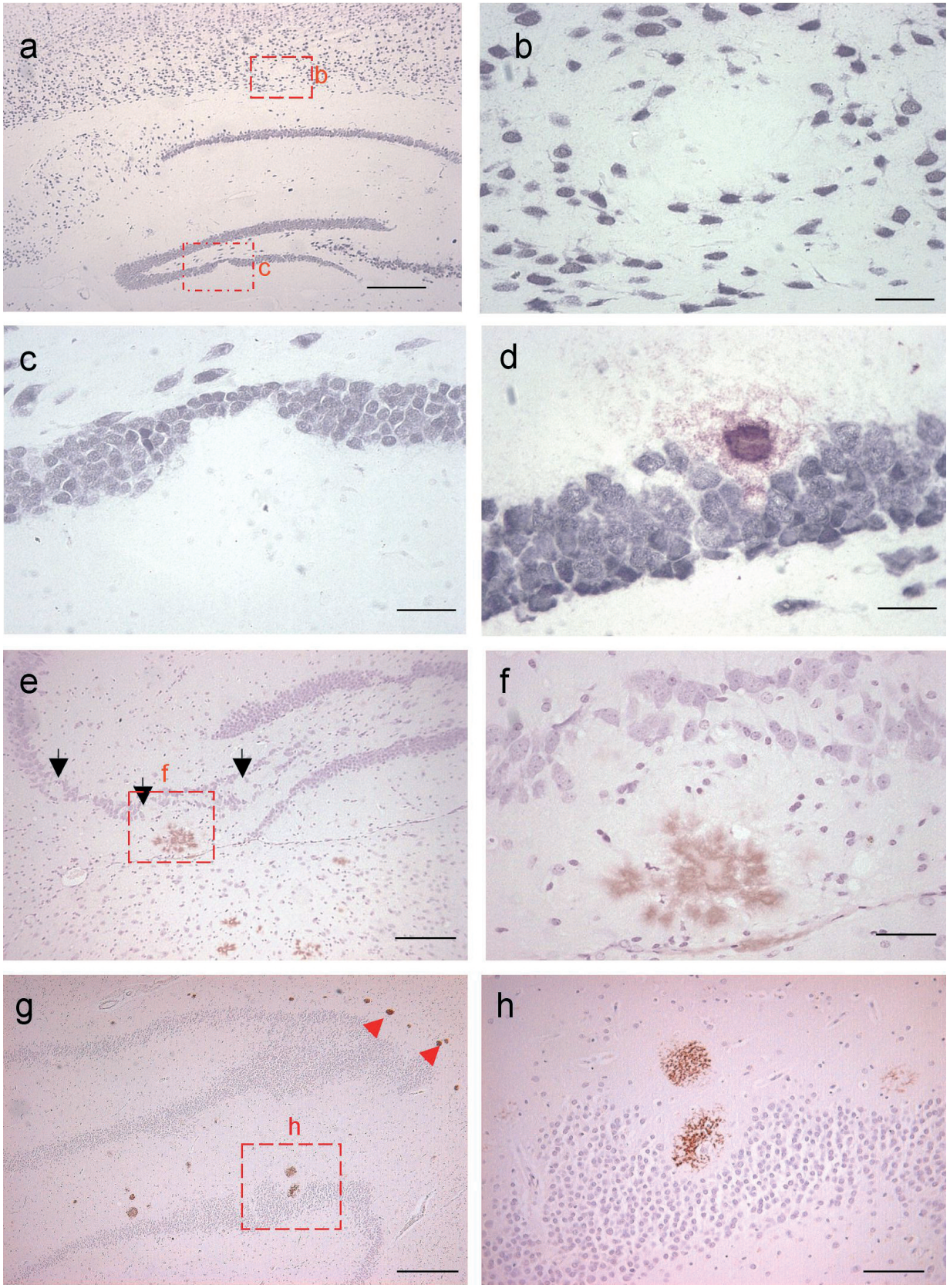

Fig. 3. Neuronal loss in the cortex and hippocampus of TASTPM mice and AD brain. **a** to **c.** NeuN (grey-blue; DAB-nickel). **b** and **c** are higher magnification images of the areas designated in (**a**). **d.** NeuN (grey-blue; DAB-nickel) plus G30 (violet; violet immunoperoxidase). **e.** pyro-3-glutamate-Aß (DAB - brown). Counterstain is Mayer's hematoxylin. Arrows show areas of neuronal loss lacking pyro-3-glutamate labelling. **f.** higher magnification of area designated in (**e**). Mice were either 44 week (**a-d**) or 80 week (**e** and **f**). **g** and **h** are AD hippocampus (Braak stage 6) with Aß42 labelling (antibody 20G10 - DAB) with Mayer's hematoxylin counterstain. **g.** arrows show a group of Aß42 positive plaques. **h.** is a higher magnification of the area designated in (**g**). Scale bars: a, 500 µm; b, c, g, 50 µm; d, 25 µm; e, 125 µm; f, 250 µm

Concentrations of Aß42 slightly exceeded those of Aß40 at the 4, 6 and 8 month time points. A basal level of GFAP labelling was observed in the cortex and hippocampus at 2 months of age although there was no significant difference between TASTPM and wild-type mice. At 4 months of age and beyond, increases in the presence of GFAP-positive astrocytes paralleled the age-related increases in Aß production, particularly in the cortex (Fig. 5b) and to a lesser extent in the hippocampus (Fig. 5c). The antibody AT8 was utilised to identify tau protein phosphorylated at the serine-202, threonine-205 epitopes (Goedert et al., 1995). AT8 immunoreactivity, in what appeared to be dystrophic neurites in close association with the Aß deposits, was apparent from 4 months of age in the cortex and hippocampus and also increased in line with the GFAP and Aß changes (Fig. 5d - f).

Discussion

In common with other APP transgenic mice, TASTPM animals exhibit an age-related increase in Aß concentration and plaque load. TASTPM mice also exhibit an apparent impairment in cognitive behaviour from around six months of age (Howlett et al., 2004). In the present study, and in agreement with previous data in TASTPM mice (Howlett et al., 2004), the Aß42 load was greater than that of Aß40. The Aß present appeared to be present in multiple oligomeric forms in plaque deposits and in surrounding tissue. Immuno-analysis of the Aß content shows the presence of multiple forms of the peptide, including full length and N-terminally truncated material, suggesting that the plaques do resemble those found in the AD brain. Furthermore, the loss of neurons observed in TASTPM mice, particularly obvious in the cell layers of the hippocampus, appears, at least histopathologically, to be of a very similar nature to that occurring in the AD brain. Although the presence of N-terminally truncated A, has been reported in AD brain (Kuo et al., 1997), its role in the pathophysiology of AD is unknown. Pyro-3-glutamate peptides have been shown to have neurotoxic properties in cell culture systems

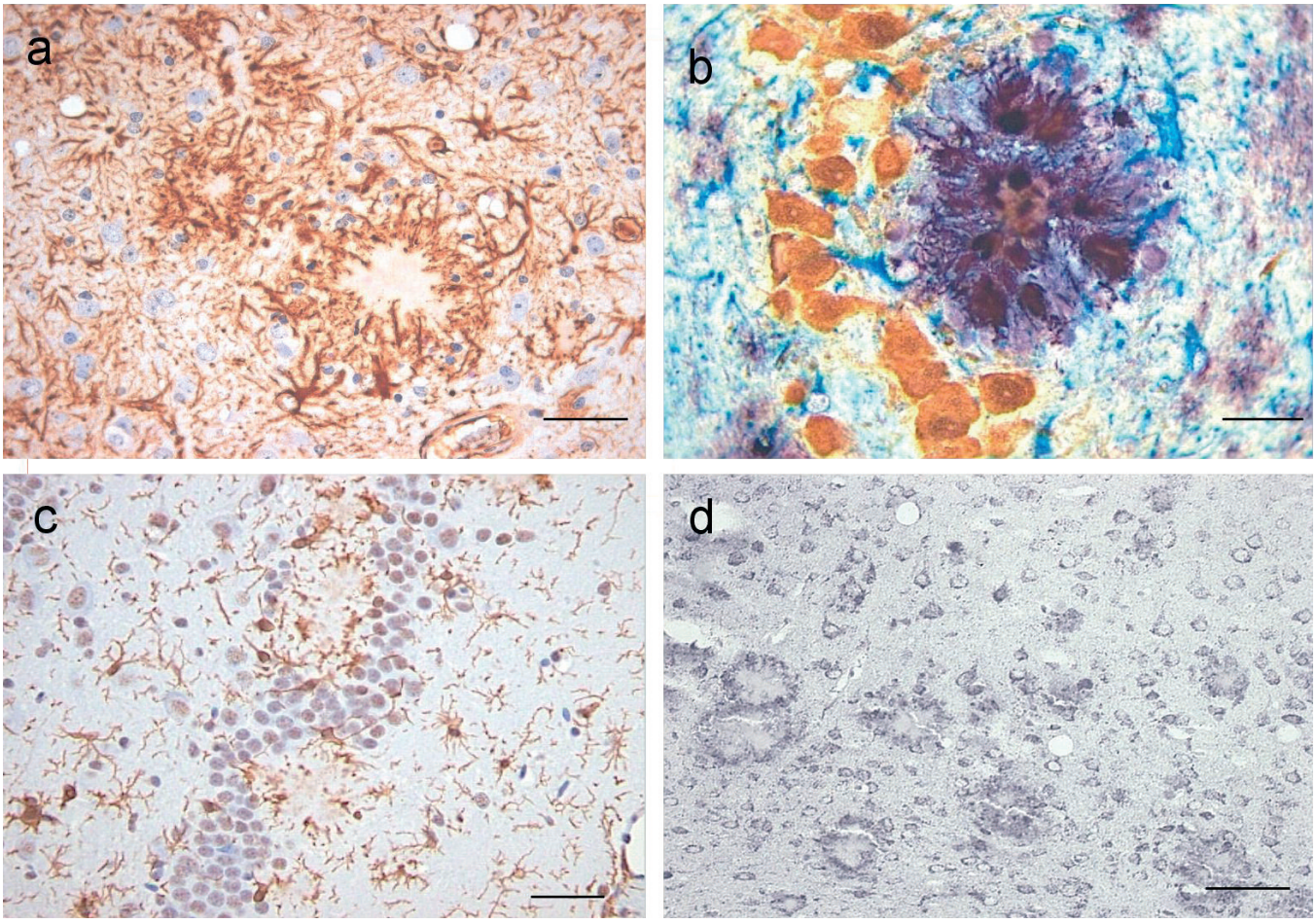

Fig. 4. Immunopathology in the cortex and hippocampus of TASTPM mice. **a.** cortical GFAP labelling (DAB). **b.** triple labelling of dentate gyrus neurons showing NeuN (brown - DAB), Aß40 (purple – violet immunoperoxidase) plus GFAP (Vector blue). **c.** iba1 (brown - DAB) with Mayer's hematoxylin counterstain. **d.** cathepsin D (DAB-nickel). Images taken from 80 week old TASTPM mice. Scale bars: a, 25 µm; b, 10 µm; c. 50 µm; d, 125 µm

(Tekirian et al., 1999). The minimal labelling with the pyro-3-glutamate antibody associated with some areas of neuronal loss in TASTPMs in the present study may suggest that this N-terminally truncated form of Aß is not essential for cell death in vivo. The presence of endogenous rodent Aß is obviously something not found in AD brain. It would appear, however, that endogenous Aß may either aggregate with the human peptide or simply adhere to the human Aß deposits. Interspecies aggregates form readily and may have increased solubility (Fung et al., 2004) but whether the presence of rodent Aß contributes to or competes against neuronal toxicity in the TASTPM brain is not known.

In AD patients, it has been reported that the degree of cognitive impairment is a function of the loss of connectivity, particularly the loss of synapses (DeKosky and Scheff, 1990). Preliminary data however has not demonstrated any comparable changes in synapse numbers in TASTPM mice at ages when cognitive impairment becomes apparent (Thaker et al., 2006 and unpublished observations). This may reflect the relatively small cognitive deficits in TASTPM mice, compared to the profound changes which occur in the latter stages of AD.

Close examination of the figures (eg. Fig. 3d) showed that thin, whispy Aß immunolabelling often filled the spaces between plaque cores and neurons. The immunohistochemical profiling of the Aß load did not provide any indication of any difference in Aß species between plaque core and immediately surrounding tissue (not shown). The resolution of laser capture microdissection (and subsequent analysis) was unable to provide the precise dissection required to separate plaque core from periphery. It was possible, however, to dissect and analyse tissue highly enriched in plaques and compare that with surrounding tissue which was, from an immunohistochemical perspective, negative for Aß. This also failed to reveal any differences in Aß species but did demonstrate the presence of SDS-stable oligomeric Aß bands, particularly between 8 and 16 kDa, in areas of tissue lacking plaques suggesting that plaques form against an underlying background of oligomerising Aß but that neuronal loss is only occurring at the points of Aß deposition, either as a result of a neurotoxic insult or simply arising from the physical presence of a deposit of foreign protein.

The role of the precise mediators of inflammation, such as interleukin-1ß and tumour necrosis factor-α, in the disease process in AD is unclear. All components of the complement system are present within the brain and both astrocytes and microglia are able to contribute to an inflammatory cascade (Owens et al., 1994). Furthermore, numerous studies have now suggested that anti-inflammatory treatments offer protection against AD (Szekely et al., 2004). The appearance of inflammatory cells in the brains of TASTPM mice

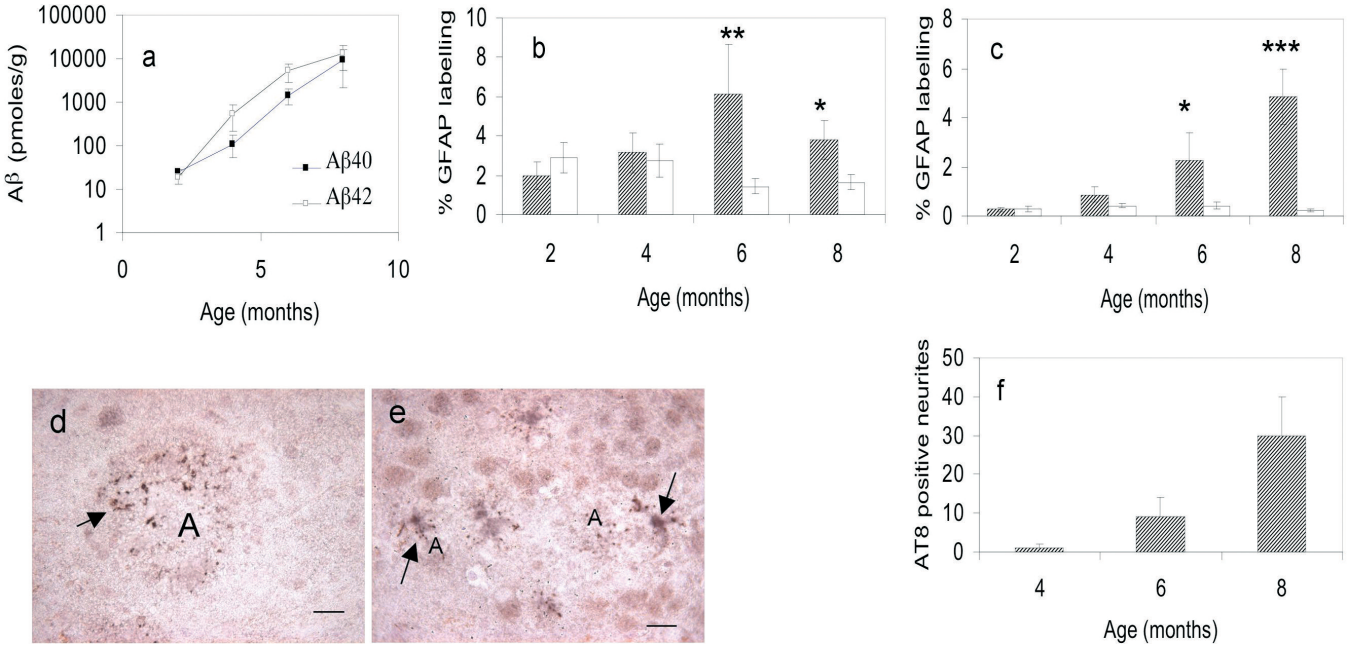

Fig. 5. Age dependent increases in brain Aß40 and 42 concentrations and in GFAP and phospho-tau labelling in TASTPM mice. **a.** Aß40 and Aß42 at 2, 4, 6 and 8 months of age. Guanidine extracts of hemisected brains from ten animals were analysed by Aß40 and 42 specific immunoassays at each time point. Quantification of GFAP immunolabelling in **(b)** hippocampus and **(c)** cortex of TASTPM (hatch columns) and wild type mice (plain columns). *p<0.05; **p<0.02; ***p<0.001 for comparisons of GFAP labelling between TASTPM and wild type mice (n=5 per group). **d-e.** Phosphotau (AT8) immunolabelling in the cortex of an 8 month old TASTPM mouse. Positively stained dystrophic neurites are arrowed. AMyloid plaques are indicated by 'A', scale bars: 15 µm. **f.** Quantification of AT8-phosphotau labelling in the cortex/hippocampus of TASTPM mice; n=6-7 per group. Wild type mice showed no AT8 labelling. x axis represents age in months.

appears to parallel the development of Aß deposits and the earliest cortical plaques, at 2-4 months of age, were accompanied by the presence of GFAP-positive astrocytes and both astrocytes and microglia were found to surround the Aß plaques. This relationship between Aß deposits and inflammatory cells has also been observed in Tg2576 transgenic mice (Frautschy et al., 1998) and both are known to be responsive to anti-inflammatory drug regimens (Lim et al., 2000). Although the effects of some non-steroidal anti-inflammatory drugs on Aß load may be a consequence of a direct effect of the drugs on APP processing (Yan et al., 2003), a direct anti-inflammatory effect, independent of Aß load, has also been demonstrated (Ranaivo et al., 2006). The exact role of astrocytes and microglia in plaque development and/or clearance is, therefore, uncertain although the close proximity of these cells to areas of Aß deposition and neuronal loss does suggest that the inflammation may be driven by the cell loss.

A major criticism of all APP transgenic mice (with or without presenilin-1 transgenes) is the lack of neurofibrillary tangles. Only when human tau transgenes are incorporated is any sign of tangle-like pathology observed (Oddo et al., 2003; Ribe et al., 2005). It has been reported that hyperphosphorylated tau-positive dystrophic neurites were observed in an APPswe x PS1.M146L double transgenic mouse (Kurt et al., 1999) and similar structures have been described elsewhere (Tomidokoro et al., 2001; Sturchler Pierrat et al., 1997). The earliest sign of hyperphosphorylated tau in TASTPM mice was observed at 4 months of age with occasional "spots" of immunoreactivity closely associated with the Aß. This phosphotau-labelling was further increased at 6 and 8 months of age and, in agreement with reports in other APP transgenic mice, appeared to be associated with dystrophic neurites. There were no obvious age-related changes in the faint intracellular phosphotau labelling and it may be unlikely that this tau contributes to the neuronal cell loss. It would appear that although Aß is somehow linked to the accumulation of phosphorylated tau in cellular structures associated with the Aß deposits, at least in the mouse, this is not sufficient to elicit tangle formation, a fact that may be reflected in the relatively minor neuronal loss in these models.

Expression and activity of cathepsins is upregulated in the CNS and is associated with leakage of lysosomal membranes with ageing. The endosomal/lysosomal system is upregulated in neurons in AD brain and this is thought to be linked to increased production of Aß in sporadic cases of AD (Nixon et al., 2000). Increases in cathepsin D activity result in increased tau phosphorylation in hippocampal slices and inhibitors of cathepsin D block the phosphorylation of tau (Bi et al., 2000). Cathepsins also mediate neuronal apoptosis and their upregulation correlates with microglial activation (Koike et al., 2003). The upregulation of cathepsin D protein in close proximity to the Aß deposits in TASTPMs would, therefore, be conducive with a role in tau phosphorylation and neuronal cell death.

The development more than a decade ago of APP transgenic mice with cortical and hippocampal Aß plaques was heralded as a major breakthrough in the quest for a rodent model of AD and their use has been fundamental to the development of potential therapies. The lack of neurofibrillary tangles and significant neuronal loss in such models, however, not only raised doubts as to their utility but also challenged the amyloid hypothesis as the driving force behind disease development and progression. Close examination of TASTPM transgenic mice and other lines such as the APP23 (Bondolfi et al., 2002) and PDAPP mice (Redwine et al., 2003) suggests that neuronal loss is occurring and that this is accompanied by tau and inflammatory pathology, albeit not on the scale observed in AD. It is also evident that despite significant Aß loads in aged APP transgenic animals cognitive manifestations are at best modest. Furthermore, although triple transgenic animals with mutant APP, PS-1 and tau transgenes do develop intracellular tangle-like phosphorylated tau inclusions (Oddo et al., 2003), a convincing representation of AD in a small mammal has yet to be demonstrated and may simply point to differences in neuronal functioning and dependency between rodents and higher mammals.

Acknowledgements. The authors would like to thank Dr Rivka Ravid, The Netherlands Brain Bank, Amsterdam, The Netherlands, for arrangement/donation of brain tissue.

References

Allsop D., Christie G., Gray C., Holmes S., Markwell R., Owen D., Smith L., Wadsworth H., Ward R.V., Hartmann T., Lichtenthaler S.F., Evin G., Fuller S., Tanner J., Masters C.L., Beyreuther K. and Roberts G.W. (1997). Studies in inhibition of ß-amyloid formation in APP 751-transfected IMR-32 cells, and SPA4CT-transfected SHSY5Y cells. In: Alzheimer's disease: Biology, diagnostics and therapeutics. Iqbal K., Winblad B., Nishimura T.,Takeda M. and Wisniewski H.M. (eds). John Wiley. New York. pp 717-727.

Bi X., Haque T.S., Zhou J., Skillman A.G., Lin B., Lee C.E., Kuntz I.D., Ellman J.A. and Lynch G. (2000). Novel cathepsin D inhibitors block the formation of hyperphosphorylated tau fragments in hippocampus. J. Neurochem. 74, 1469-1477.

Bondolfi L., Calhoun M., Ermini F., Kuhn H.G., Wiederhold K.H., Walker L., Staufenbiel M. and Jucker M. (2002). Amyloid-associated neuron loss and gliogenesis in the neocortex of amyloid precursor protein transgenic mice. J. Neurosci. 22, 515-522.

Borchelt D.R., Ratovitski T., Vanlare J., Lee M.K., Gonzales V., Jenkins N.A., Copeland N.G., Price D.L. and Sisodia S.S. (1997). Accelerated amyloid deposition in the brains of transgenic mice coexpressing mutant presenilin-1 and amyloid precursor proteins. Neuron 19, 939-945.

Braak H., Rüb U., Schultz C. and Del Tredici K. (2006). Vulnerability of cortical neurons to Alzheimer's and Parkinson's diseases. J. Alz. Dis. 9, 35-44.

Chishti M.A., Yang D.S., Janus C., Phinney A.L., Horne P., Pearson J.,

Strome R., Zuker N., Loukides J., French J., Turner S., Lozza G., Grilli M., Kunicki S., Morissette C., Paquette J., Gervais F., Bergeron C., Fraser P.E., Carlson G.A., George-Hyslop P. and Westaway D. (2001). Early-onset amyloid deposition and cognitive deficits in transgenic mice expressing a double mutant form of amyloid precursor protein 695. J. Biol. Chem. 276, 21562-21570.

DeKosky S.T. and Scheff S.W. (1990). Synapse loss in frontal cortex biopsies in Alzheimer's disease: correlation with cognitive severity. Ann. Neurol. 27, 457-464.

Dewachter I., Van Dorpe J., Smeijers L., Gilis M., Kuiperi C., Laenen I., Caluwaerts N., Moechars D., Checler D.R., Vanderstichele H. and Van Leuven F. (2000). Aging increased amyloid peptide and caused amyloid plaques in brain of old APP/V717I transgenic mice by a different mechanism than mutant presenilin1. J. Neurosci. 20, 6452-6458.

Frautschy S.A., Yang F., Irrizarry M., Hyman B., Saido T.C., Hsiao K. and Cole G. M. (1998). Microglial response to amyloid plaques in APPsw transgenic mice. Am. J. Pathol. 152, 307-317.

Fung J., Frost D., Chakrabartty A. and McLaurin J.A. (2004). Interaction of human and mouse A beta peptides. J. Neurochem. 91, 1398-1403.

Games D., Adams D., Alessandrini R., Barbour R., Berthelette P., Blackwell C., Carr T., Clemens J., Donaldson T., Gillespie F., Guido T., Hagopian S., Johnsonwood K., Khan K., Lee M., Leibowitz P., Lieberburg I., Little S., Masliah E., McConlogue L., Montoyazavala M., Mucke L., Paganini L., Penniman E., Power M., Schenk D., Seubert P., Snyder B., Soriano F., Tan H., Vitale J., Wadsworth S., Wolozin B. and Zhao J. (1995). Alzheimer-type neuropathology in transgenic mice overexpressing v717f beta-amyloid precursor protein. Nature 373, 523-527.

Goedert M., Jakes R. and Vanmechelen E. (1995). Monoclonal antobody AT8 recognises tau protein phosphorylated at the serine 202 and threonine 205 epitopes. Neurosci. Lett. 189, 167-70.

Holcomb L., Gordon M.N., Mcgowan E., Yu X., Benkovic S., Jantzen P., Wright K., Saad I., Mueller R., Morgan D., Sanders S., Zehr C., O'Campo K., Hardy J., Prada C.M., Eckman C., Younkin S., Hsiao K. and Duff K. (1998). Accelerated Alzheimer-type phenotype in transgenic mice carrying both mutant amyloid precursor protein and presenilin 1 transgenes. Nat. Med. 4, 97-100.

Howlett D.R., Richardson J.C., Austin A., Parsons A.A., Bate S.T., Davies D.C. and Gonzalez M.I. (2004). Cognitive correlates of Abeta deposition in male and female mice bearing amyloid precursor protein and presenilin-1 mutant transgenes. Brain Res. 1017,130-136.

Hsiao K., Chapman P., Nilsen S., Eckman C., Harigaya Y., Younkin S., Yang F. and Cole G. (1996). Correlative memory deficits, Abeta elevation, and amyloid plaques in transgenic mice. Science 274, 99-102.

Kawarabayashi T., Younkin L.H., Saido T.C., Shoji M., Ashe K.H. and Younkin S.G. (2001). Age-dependent changes in brain, CSF, and plasma amyloid beta protein in the Tg2576 transgenic mouse model of Alzheimer's disease. J. Neurosc. 21, 372-381.

Koike M., Shibata M., Ohsawa Y., Nakanishi H., Koga T., Kametaka S., Waguri S., Momoi T., Kominami E., Peters C., Figura K., Saftig P. and Uchiyama Y. (2003). Involvement of two different cell death pathways in retinal atrophy of cathepsin D-deficient mice. Mol. Cell. Neurosci. 22, 146-161.

Kuo Y.M., Emmerling M.R., Woods A.S., Cotter R.J. and Roher A.E. (1997). Isolation, chemical characterization, and quantitation of A beta 3-pyroglutamyl peptide from neuritic plaques and vascular amyloid deposits. Biochem. Biophys. Res. Commun. 237, 188-191.

Kurt M.A., Davies D.C. and Kidd M. (1999). beta-Amyloid immunoreactivity in astrocytes in Alzheimer's disease brain biopsies: an electron microscope study. Exp. Neurol. 158, 221-228.

Kurt M.A., Davies D.C., Kidd M., Duff K., Rolph S.C., Jennings K.H. and Howlett D.R. (2001). Neurodegenerative changes associated with beta-amyloid deposition in the brains of mice carrying mutant amyloid precursor protein and mutant presenilin-1 transgenes. Exp. Neurol. 171, 59-71.

Lim G.P., Yang F., Chu T., Chen P., Beech W., Teter B., Tran T., Ubeda O., Ashe K.H., Frautschy S.A. and Cole G.M. (2000). Ibuprofen suppresses plaque pathology and inflammation in a mouse model for Alzheimer's disease. J. Neurosci. 20, 5709-5714.

Mann D.M. (1991). The topographic distribution of brain atrophy in Alzheimer's disease. Acta Neuropathol. 83, 81-86.

Mouton P.R., Martin L.J., Calhoun M.E., Dal Forno G. and Price D.L., (1998). Cognitive decline strongly correlates with cortical atrophy in Alzheimer's dementia. Neurobiol. Aging 19, 371-3777

Nixon R.A., Cataldo A.M. and Mathews P.M. (2000). The endosomal-lysosomal system of neurons in Alzheimer's disease pathogenesis: A review. Neurochem. Res. 25, 1161-1172.

Oddo S., Caccamo A., Shepherd J.D., Murphy M.P., Golde T.E., Kayed R., Metherate R., Mattson M.P., Akbari Y. and Laferla F.M. (2003). Triple-transgenic model of Alzheimer's disease with plaques and tangles: Intracellular A beta and synaptic dysfunction. Neuron 39, 409-421.

Owens T., Renno T., Taupin V. and Krakowski M. (1994). Inflammatory cytokines in the brain: does the CNS shape immune responses? Immunol. Today 15, 566-570.

Ranaivo H.R., Craft J.M., Hu W.H., Guo L., Wing L.K., Van Eldik L.J. and Watterson D.M. (2006). Glia as a therapeutic target: Selective suppression of human amyloid-beta-induced upregulation of brain proinflammatory cytokine production attenuates neurodegeneration. J. Neurosci. 26, 662-670.

Redwine J.M., Kosofsky B., Jacobs R.E., Games D., Reilly J.F., Morrison J.H., Young W.G. and Bloom F.E. (2003). Dentate gyrus volume is reduced before onset of plaque formation in PDAPP mice: A magnetic resonance microscopy and stereologic analysis. Proc. Natl. Acad. Sci. USA 100, 1381-1386.

Ribe E.M., Perez M., Puig B., Gich I., Lim F., Cuadrado M., Sesma T., Catena S., Sanchez B., Nieto M., Gomez-Ramos P., Moran M.A., Cabodevilla F., Samaranch L., Ortiz L., Perez A., Ferrer I., Avila J. and Gomez-Isla T. (2005). Accelerated amyloid deposition, neurofibrillary degeneration and neuronal loss in double mutant APP/tau transgenic mice. Neurobiol. Dis. 20, 814-822.

Richardson J.C., Kendal C.E., Anderson R., Priest F., Gower E., Soden P., Gray R., Topps S., Howlett D.R., Lavender D., Clarke N.J., Barnes J.C., Haworth R., Stewart M.G. and Rupniak H.T.R. (2003). Ultrastructural and behavioural changes precede amyloid deposition in a transgenic model of Alzheimer's disease. Neuroscience 122, 213-228.

Schmitz C., Rutten B.P.F., Pielen A., Schafer S., Wirths O., Tremp G., Czech C., Blanchard V., Multhaup G., Rezaie P., Korr H., Steinbusch H.W.M., Pradier L. and Bayer T.A. (2004). Hippocampal neuron loss exceeds amyloid plaque load in a transgenic mouse model of Alzheimer's disease. Am. J. Pathol. 164, 1495-1502.

Selkoe D.J. and Podlisny M.B. (2002). Deciphering the genetic basis of

Alzheimer's disease. Annu. Rev. Genom. Hum. Gen. 3, 67-99.

Sturchler Pierrat C., Abramowski D., Duke M., Wiederhold K.H., Mistl C., Rothacher S., Ledermann B., Burki K., Frey P., Paganetti P.A., Waridel C., Calhoun M.E., Jucker M., Probst A., Staufenbiel M. and Sommer B. (1997). Two amyloid precursor protein transgenic mouse models with Alzheimer disease-like pathology. Proc. Natl. Acad. Sci. USA 94, 13287-13292.

Szekely C.A., Thorne J.E., Zandi P.P., Ek M., Messias E., Breitner J.C. and Goodman S.N. (2004). Nonsteroidal anti-inflammatory drugs for the prevention of Alzheimer's disease: a systematic review. Neuroepid. 23, 159-169.

Tekirian T.L., Yang A.Y., Glabe C. and Geddes J.W. (1999). Toxicity of pyroglutaminated amyloid beta-peptides 3(pE)-40 and-42 is similar to that of A beta 1-40 and-42. J. Neurochem. 73, 1584-1589.

Thaker U., Howlett D.R. and Davies D.C. (2006). A decrease in cortical synapse density does not appear to underlie early cognitive deficits in the TASTPM mouse model of Alzheimer's disease. Alz. Dementia 2, S109.

Tomidokoro Y., Harigaya Y., Matsubara E., Ikeda M., Kawarabayashi T., Shirao T., Ishiguro K., Okamoto K., Younkin S.G. and Shoji M. (2001). Brain A beta amyloidosis in APPsw mice induces accumulation of presenilin-I and tau. J. Pathol. 194, 500-506.

Yan Q., Zhang J.H., Liu H.T., Babu-Khan S., Vassar R., Biere A.L., Citron M. and Landreth G. (2003). Anti-inflammatory drug therapy alters beta-amyloid processing and deposition in an animal model of Alzheimer's disease. J. Neurosci. 23, 7504-7509.

Accepted July 11, 2007